



Co-targeting of FAK and MDM2 triggers additive anti-proliferative effects in mesothelioma via a coordinated reactivation of p53

The Harvard community has made this article openly available. [Please share](#) how this access benefits you. Your story matters

Citation	Ou, W., M. Lu, G. Eilers, H. Li, J. Ding, X. Meng, Y. Wu, et al. 2016. "Co-targeting of FAK and MDM2 triggers additive anti-proliferative effects in mesothelioma via a coordinated reactivation of p53." British Journal of Cancer 115 (10): 1253-1263. doi:10.1038/bjc.2016.331. http://dx.doi.org/10.1038/bjc.2016.331 .
Published Version	doi:10.1038/bjc.2016.331
Citable link	http://nrs.harvard.edu/urn-3:HUL.InstRepos:34493147
Terms of Use	This article was downloaded from Harvard University's DASH repository, and is made available under the terms and conditions applicable to Other Posted Material, as set forth at http://nrs.harvard.edu/urn-3:HUL.InstRepos:dash.current.terms-of-use#LAA

Keywords: FAK; p53; MDM2; NF2; mesothelioma

Co-targeting of FAK and MDM2 triggers additive anti-proliferative effects in mesothelioma via a coordinated reactivation of p53

Wen-Bin Ou^{*1,2,3}, Minmin Lu¹, Grant Eilers², Hailong Li³, Jiongyan Ding¹, Xuli Meng⁴, Yuehong Wu¹, Quan He¹, Qing Sheng¹, Hai-Meng Zhou³ and Jonathan A Fletcher²

¹Zhejiang Provincial Key Laboratory of Silkworm Bioreactor and Biomedicine, College of Life Sciences, Zhejiang Sci-Tech University, Hangzhou, China; ²Department of Pathology, Brigham and Women's Hospital and Harvard Medical School, Boston, MA, USA; ³Zhejiang Provincial Key Laboratory of Applied Enzymology, Yangtze Delta Region Institute of Tsinghua University, Jiaying, Zhejiang, China and ⁴Department of Breast Cancer Surgery, Zhejiang Cancer Hospital, Hangzhou, China

Background: Improved mesothelioma patient survival will require development of novel and more effective pharmacological interventions. *TP53* genomic mutations are uncommon in mesothelioma, and recent data indicate that p53 remains functional, and therefore is a potential therapeutic target in these cancers. In addition, the tumour suppressor NF2 is inactivated by genomic mechanisms in more than 80% of mesothelioma, causing upregulation of FAK activity. Because FAK is a negative regulator of p53, NF2 regulation of FAK–p53–MDM2 signalling loops were evaluated.

Methods: Interactions of FAK–p53 or NF2–FAK were evaluated by phosphotyrosine-p53 immunoaffinity purification and tandem mass spectrometry, and p53, FAK, and NF2 immunoprecipitations. Activation and/or expression of FAK, p53, and NF2 were also evaluated in mesotheliomas. Effects of combination MDM2 and FAK inhibitors/shRNAs were assessed by measuring mesothelioma cell viability/growth, expression of cell cycle checkpoints, and cell cycle alterations.

Results: We observed constitutive activation of FAK, a known negative regulator of p53, in each of 10 mesothelioma cell lines and each of nine mesothelioma surgical specimens, and FAK was associated with p53 in five of five mesothelioma cell lines. In four mesotheliomas with wild-type p53, FAK silencing by RNAi induced expression and phosphorylation of p53. However, FAK regulation of mesothelioma proliferation was not restricted to p53-dependent pathways, as demonstrated by immunoblots after FAK knockdown in JMN1B mesothelioma cells, which have mutant/inactivated p53, compared with four mesothelioma cell lines with nonmutant p53. Additive effects were obtained through a coordinated reactivation of p53, by FAK knockdown/inhibition and MDM2 inhibition, as demonstrated by immunoblots, cell viability, and cell-cycle analyses, showing increased p53 expression, apoptosis, anti-proliferative effects, and cell-cycle arrest, as compared with either intervention alone. Our results also indicate that NF2 regulates the interaction of FAK–p53 and MDM2–p53.

Conclusions: These findings highlight novel therapeutic opportunities in mesothelioma.

Mesothelioma is a locally aggressive and highly lethal neoplasm, linked epidemiologically to asbestos exposure (Craighead and Mossman, 1982; Jongsma *et al*, 2008), and SV40 virus infection (Carbone *et al*, 1994), in which the neoplastic proliferation originates from pleural, peritoneal, or – rarely – pericardial mesothelial cells. Pathologically, mesothelioma histological

*Correspondence: Dr W-B Ou; E-mail: ouwenbin@tsinghua.org.cn or Dr JA Fletcher; E-mail: jfletcher@partners.org

Received 28 June 2016; revised 12 September 2016; accepted 21 September 2016; published online 13 October 2016

© 2016 Cancer Research UK. All rights reserved 0007–0920/16

subtypes are epithelioid, spindle-cell, and mixed (epithelioid and spindled; Janne *et al*, 2002), of which the spindled type has the worst prognosis. Conventional chemotherapies and radiation therapy have limited efficacy against mesothelioma, and substantial improvements in survival will require development of novel and more effective pharmacological interventions. A better understanding of mesothelioma biology – including the function of highly recurrent mutations such as NF2 (Bianchi *et al*, 1995) and BAP1 (Bott *et al*, 2011; Testa *et al*, 2011), and key growth factor signalling pathways – will likely be useful in identifying biologically rational targets for novel therapies.

Focal adhesion kinase (FAK) is a non-receptor tyrosine kinase that mediates signalling through several downstream pathways, leading to cell migration, growth factor signalling, cell cycle progression, and cell survival (Lim *et al*, 2008; Ding *et al*, 2010; Huang *et al*, 2010; Long *et al*, 2010). Furthermore, FAK has a prominent role in integrin and receptor tyrosine kinase (RTK) signalling (Parsons, 2003). Although FAK itself has not been demonstrated to be an oncogene, FAK overexpression has been reported in tumours of various tissue origins, especially in invasive and metastatic tumours (Gabarra-Niecko *et al*, 2003). The effects of FAK on tumour growth in mice suggest that FAK may influence the formation, growth, and metastasis of tumours (Gabarra-Niecko *et al*, 2003; Slack-Davis *et al*, 2009). There is increasing evidence to indicate that FAK has an important role in regulating cell cycle progression through cyclin D1 transcription, p27 expression, and MAPK activation (Zhao *et al*, 2001; Ding *et al*, 2005). The tumour suppressor p53 was first linked with FAK by Ilic *et al* (Ilic *et al*, 1998) and a p53 binding site has been identified in the FAK promoter (Golubovskaya *et al*, 2004). Recently, studies of direct interaction of the N-terminal domain of FAK with the N-terminal transactivation domain of p53, particularly at the 7-amino-acid site in the proline-rich region of the p53 N-terminal domain, indicated that FAK can suppress p53-mediated apoptosis and inhibit the transcriptional activity of p53 (Golubovskaya *et al*, 2005; Golubovskaya *et al*, 2008). FIP200, a FAK inhibitor, has been shown to induce cell cycle arrest by increasing the expression and phosphorylation of p53 in human breast cancer cells (Melkoumian *et al*, 2005). FAK inactivates p53 in a kinase-independent manner through the FAK FERM domain, which acts as a scaffold to enhance MDM2-dependent p53 ubiquitination. Importantly, p53 regulation is dependent on FAK nuclear translocation (Lim *et al*, 2008). These observations suggest that FAK regulates cell cycle progression in a p53-dependent manner. However, it is still unclear whether the FAK–p53 cell survival pathway may also have a role in promoting tumour progression.

Mouse double minute 2 (MDM2) is an oncoprotein, the primary E3 ubiquitin ligase responsible for ubiquitination and degradation of p53 (Brooks and Gu, 2006). The structure of MDM2 bound to p53 and the molecular mechanisms of the interaction between MDM2 and p53 have been well characterised (Kussie *et al*, 1996; Schon *et al*, 2002; Chene, 2003; White *et al*, 2006). Thus, inhibition of the MDM2–p53 interaction by small molecules is an attractive therapeutic opportunity in oncology. Nutlin-3, a specific small-molecule inhibitor of MDM2, suppresses the interaction of MDM2 with wild-type p53, activating its anticancer activity (Kojima *et al*, 2006; Tovar *et al*, 2006; Van *et al*, 2009; Moran and Maki, 2010). Nutlin-3 shows strong antitumour effects in mice, with few side effects on normal tissues (Brummelkamp *et al*, 2006), indicating that tumours with wild-type p53 may be susceptible to inhibition of the MDM2–p53 interaction. Recently, we found that wild-type p53 depletion by histone deacetylase inhibitors was MDM2 amplification-dependent (Ou *et al*, 2015), and inhibition of PI3K/AKT was also associated with MDM2–p53 cell cycle regulation (Zhou *et al*, 2014).

TP53 mutations are seen infrequently in mesothelioma (Metcalf *et al*, 1992; Papp *et al*, 2001). Recent data also indicate that p53 is

functional in the absence of p14ARF and, if reactivated, can induce apoptosis in mesothelioma (Hopkins-Donaldson *et al*, 2006). Suppressor of cytokine signalling 3 (SOCS3) overexpression showed anti-proliferative effects in mesotheliomas via multiple signalling pathways including JAK/STAT3 and FAK/p53 (Iwahori *et al*, 2011). Increasing p53 expression enhances cytotoxicity of the first-line chemotherapeutics cisplatin or pemetrexed in p53-wild-type mesothelioma (Li *et al*, 2012).

The NF2 (merlin) is a tumour-suppressor protein, inactivated by genomic mechanisms in more than 80% of mesothelioma; these are crucial events in mesothelioma pathogenesis, and result in hyperactivation of FAK (Bianchi *et al*, 1995; Poulikakos *et al*, 2006). Recent studies showed that NF2 deficiency predicts increased sensitivity of mesothelioma cells to a FAK inhibitor, VS-4718 (Shapiro *et al*, 2014). In addition, previous data have demonstrated that NF2 neutralises the inhibitory effect of MDM2 on p53 (Kim *et al*, 2004).

In the present study, we investigated interaction of FAK and p53 through a functional proteomic approach including phosphotyrosine and p53 immunoprecipitation double immunoaffinity purification, and tandem mass spectrometry. The expression and phosphorylation of FAK and p53 were also evaluated in mesothelioma cell lines and primary tumours. We evaluated the effects of coordinated reactivation of p53, and our findings highlight novel therapeutic opportunities in mesothelioma.

MATERIALS AND METHODS

Antibodies and reagents. Polyclonal antibody to FAK, and monoclonal antibodies to phosphotyrosine (PY99), p53, PARP, and NF2 were from Santa Cruz Biotechnology (Santa Cruz, CA, USA). Monoclonal mouse antibodies to MDM2 and p21, and polyclonal antibody to phospho-FAK (Y397) were from Zymed Laboratories (Invitrogen Life Technologies, Carlsbad, CA, USA). Polyclonal antibodies to phospho-p53 (Ser15) and phospho-NF2 (Ser518) were from Cell Signaling Technology (Beverly, MA, USA). Phospho-FAK (Y861) was obtained from Biosource (Invitrogen Life Technologies). We obtained monoclonal mouse antibodies to cyclin A from Novocastra (Newcastle upon Tyne, UK), and β -actin and GAPDH from Sigma-Aldrich (St Louis, MO, USA).

Mouse anti-phosphotyrosine (PY)-sepharose 4B, Protein A- and Protein G-sepharose beads were from Zymed Laboratories. NOVEX Coomassie colloidal blue stain kit, NuPAGE TM 4–12% Bis-Tris Gel, Lipofectamine and Plus reagent were obtained from Invitrogen Life Technologies. Phenyl phosphate and polybrene were from Sigma. Nutlin-3 and PF562271 were obtained from LC Labs (Woburn, MA, USA) and Symansis (Auckland, NZ, USA), respectively. Lentiviral *NF2 shRNAs* were from Sigma. *NF2 shRNA1*: 5'-CCGGCGGGCTTTGTTTCCTTCTTTACTCGAGTAAGAAGGAAACAAAGCCCGTTTTGTG-3'; *NF2 shRNA2*: 5'-CCGGCTTCGTGTTAATAAGCTGATCTCGAGATCAGCTTATTAACACGAAGCTTTTGTG-3'.

Mesothelioma cell lines and frozen tumour specimens. Eight mesothelioma cell lines were established from surgical materials from previously untreated patients, as reported previously (Ou *et al*, 2011). The MESO59, MESO257, MESO542, and MESO924 cell lines were established from epithelial-type mesotheliomas, MESO296, MESO589, and MESO647 from mixed-histology mesotheliomas, and MESO428 from a spindle-cell mesothelioma. An additional mesothelioma cell line, JMN1B, was established from an epithelial-type mesothelioma (Demetri *et al*, 1989). Derivation of each cell line from the corresponding surgical specimen was corroborated by STR profiling (Supplementary Table 1). All mesothelioma frozen tumour specimens were discarded tissues, obtained from Brigham and Women's Hospital. The Brigham and Women's Hospital

Institutional Review Board approved the experiments, and informed consent was obtained from all the subjects.

Phosphotyrosine-p53 immunoprecipitation and tandem mass spectrometry. Tyrosine kinases (TKs) were immunoprecipitated from mesothelioma cell lysates using a p53 monoclonal antibody, and subsequently immunoblotted and stained for phosphotyrosine (PY99) to identify the molecular mass of putative activated TKs, which interacted with p53. Candidate-activated TKs were then characterised from the MESO257 cell line by mass spectrometry. Activated proteins were purified on a phosphotyrosine (PY) immunoaffinity column in which 0.5 ml of sepharose-conjugated anti-PY was loaded in a 10 ml polypropylene column and washed with a 5X volume of 1 × PBS containing 0.02% sodium azide. The column was pre-equilibrated with a 5X volume of lysis buffer, then incubated with 10 mg of protein lysates at 4 °C with overnight end-over-end mixing. The flow-through fraction was collected and reloaded on the column 10 times. The column was then washed with 1 ml lysis buffer five times, and the tyrosine-phosphorylated proteins were eluted with 1 ml 100 mM phenyl phosphate in lysis buffer 10 times. The eluates were dialysed against 1 litre of 1 × PBS buffer overnight at 4 °C. The sample was then concentrated to ~100 µl of final volume using centricon filters (Millipore Corporation, Bedford, MA, USA). Ninety-six percent of the eluates were immunoprecipitated by antibody to p53. Finally, 4% of the eluates and 15% of the PY-p53 fractions were immunoblotted and stained for phosphotyrosine, while the remaining 85% of the PY-p53 fractions were gel electrophoresed and stained using a NOVEX Coomassie colloidal blue stain kit protocol. A strongly phosphorylated protein band at 130 kDa was excised from the Coomassie gel, and protein sequences were determined by mass spectrometry. The blots were then stripped and restained with specific antibodies to validate candidate tyrosine kinases.

Western blotting analysis. Whole-cell lysates were prepared using lysis buffer (1% NP-40, 50 mM Tris-HCl pH 8.0, 100 mM sodium fluoride, 30 mM sodium pyrophosphate, 2 mM sodium molybdate, 5 mM EDTA, and 2 mM sodium orthovanadate) containing protease inhibitors (10 µg ml⁻¹ aprotinin, 10 µg ml⁻¹ leupeptin, and 1 mM phenylmethylsulfonyl fluoride). Frozen tumour samples were diced into small pieces in cold lysis buffer on dry ice and homogenised using a Tissue Tearor (Model 398, Biospec Products, Inc., Bartlesville, OK, USA) for 2 s, —three to five times, on ice, and the cell lysate was then rocked overnight at 4 °C. The lysates were cleared by centrifugation at 14 000 g for 20 min at 4 °C, and lysate protein concentrations were determined using a Bio-Rad protein assay (Bio-Rad Laboratories Hercules, CA, USA). Nuclear, membrane, and cytoplasmic fraction lysates were prepared by using a Qproteome Cell Compartment Kit (Qiagen Inc., Valencia, CA, USA) according to the manufacturer's protocol. Electrophoresis and western blotting were performed as described previously (Rubin *et al.*, 2001). The hybridisation signals were detected by chemiluminescence (ECL, Amersham Pharmacia Biotechnology, Marlborough, MA, USA) and captured using a FUJI LAS1000-plus chemiluminescence imaging system.

Immunoprecipitation. Sepharose-protein A to rabbit polyclonal antibodies and Sepharose-protein G to mouse monoclonal antibodies were used. One milligram of protein lysates (500 µl) was preadsorbed for 30 min using 20 µl of protein A or protein G beads at 4 °C. Two micrograms of primary antibodies against FAK, p53, or NF2 were rocked with the lysates for 2 h at 4 °C. Then 20 µl of sepharose-protein A or -protein G beads were added and rocked overnight at 4 °C, then centrifuged at 10 000 g for 2 min at 4 °C, after which the sepharose beads were washed three times with 750 µl of IP buffer (25 min each time) and once with 750 µl 10 mM

Tris-Cl buffer (pH 7.6). Loading buffer (20 µl) was added to the beads and boiled for 5 min at 95 °C.

Lentiviral FAK shRNA constructs and virus preparation. The pLKO.1puro (7 kb) lentivirus construct contains an U6 promoter and HIV-1 RNA packaging signal with a puromycin- and ampicillin-resistant element cloned 3' of the human phosphoglycerate kinase (hPGK) promoter. A cpptCTE was inserted 5' of the hPGK promoter. Human FAK shRNA constructs were generated by ligating the following oligomers into the unique *AgeI* and *EcoRI* sites of pLKO.1puro: FAK forward 5'-CCGGCCGGTCGAATGATAAGGTGACTCGAGTACACCTTATCATTTCGACCCGGTTTTTG-3' and reverse 5'-AATTCAAAAACCGGTGCAATGATAAGGTGACTCGAGTACACCTTATCATTTCGACCCGG-3'.

Lentivirus preparations were produced by cotransfecting pLKO.1puro with FAK or NF2 shRNA and helper virus packaging plasmids pCMVΔR8.91 and pMD.G (at a 10:10:1 ratio) into 293T cells. Transfections were carried out using Lipofectamine and PLUS reagent. Lentiviruses were harvested at 24, 36, 48, and 60 h post transfection. The virus was frozen at -80 °C in appropriately sized aliquots for infection. Well-validated shRNAs were used for FAK and NF2 knockdowns.

Cell culture and virus infection. Mesothelioma cells were cultured in RPMI 1640 media with 15% fetal bovine serum (FBS) and seeded in six-well plates. Lentiviral shRNA infections were carried out in the presence of 8 µg ml⁻¹ polybrene. The cells were lysed for western blot analysis or harvested for cell cycle analysis at 96 h post infection. The MESO257 cells were selected for stable expression of the NF2 shRNAs using 2 µg ml⁻¹ puromycin.

Cell viability analysis. MESO924, MESO257, MESO296, MESO428, JMN1B, and stably infected MESO257 with NF2 shRNA knockdown were plated at 3000 cells per well in a 96-well flat-bottomed plate (Falcon, Lincoln, NJ, USA) and cultured in RPMI 1640 for 24 h before transduction with lentiviral empty vector or FAK shRNA, or treatment with MDM2 inhibitor nutlin-3 and FAK inhibitor PF562271, or 48 h before treatment with nutlin-3 after FAK shRNA transduction. Proliferation studies were carried out after 3 or 6 days using the CellTiter-Glo luminescent assay from Promega (Madison, WI, USA), and quantified using a Veritas Microplate Luminometer from Turner Biosystems (Sunnyvale, CA, USA). The data were normalised to the empty vector group or DMSO. All the assays were performed in quadruplicate wells, and were averaged from two independent experiments for each cell line.

Cell cycle analysis. MESO924, MESO257, MESO296, MESO428, and JMN1B cells in six-well plates were trypsinised and washed with Hanks Balanced Salt Solution at room temperature after infection with lentivirus for 72 h and/or treatment with nutlin-3 for 48 h. For nuclear staining, a DAPI-containing solution (nuclear isolation and staining solution, NPE systems, Pembroke Pines, FL) was added to the cells and the cell suspension was immediately analysed in a flow cytometer (NPE Quanta, NPE Systems). Data analyses were performed using Modfit LT software 3.1 (Verity Software House, Topsham, ME, USA).

NF2 S518 point mutagenesis. Human NF2 full-length cDNA expression plasmid (Catalogue: TC124024) was obtained from Origene (Rockville, MD, USA). QuikChange Lightning Site-Directed Mutagenesis Kit was from Agilent Technologies (Santa Clara, CA, USA). NF2 S518A forward primer: 5'-actgacatgaagcggcttgcctgagatagaga-3' reverse primer: 5'-tctctatctcctgcaagccgcttcattgctcagt-3' NF2 S518D forward primer: 5'-aagatactgacatgaagcggcttcacatgagatagagaagaaaag-3' reverse primer: 5'-cttttcttctctatctcattgctcagccgcttcattgctcagtatctt-3'. The NF2 mutation was validated by sequencing.

Statistical analysis. Student's *t*-tests were performed on data from cells treated with control DMSO or inhibitors, as well as cells treated with empty vector or *FAK shRNA*. Statistically significant differences between untreated control and treatment were defined as **P*<0.05, ***P*<0.01, and ****P*<0.001.

RESULTS

FAK non-receptor tyrosine kinase is strongly activated and interacts with p53 in mesothelioma. Phosphotyrosine eluates, phosphotyrosine-p53 fractions, and p53 immunoprecipitations were prepared from the MESO257 cell line, and phosphotyrosine stains demonstrated ~130 kDa proteins in immunoblot preparations (Figure 1). Mass spectrometry analysis of the ~130 kDa band cut from a Coomassie-stained gel identified the FAK non-receptor tyrosine kinase. This finding was confirmed by subsequent stripping of the immunoblots and restaining for FAK (Figure 1). The p53 immunoblotting was not shown because of overlay of p53 and immunoglobulin heavy chain.

Using MESO924 as an internal standard, the phosphorylation and expression of FAK and p53 were evaluated by immunoblotting in mesothelioma cell lines and primary tumours. FAK and p53 were

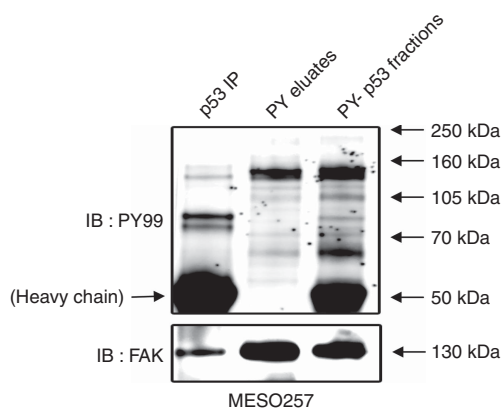


Figure 1. FAK phosphorylation and expression in MESO257 as evaluated by phosphotyrosine (PY) and FAK staining of immunoblots. FAK is associated with p53 in p53 immunoprecipitation (lane 2) and appears in the MESO257 phosphotyrosine fraction (lane 4). Size-based identifications (PY99 stain) were corroborated by mass spectrometry (data not shown).

expressed in most mesotheliomas, with especially strong expression of p53 in JMN1B and one frozen tumour, both of which have been found to contain *TP53* missense mutations (JMN1B: G245S; MESO96–975: A159V) (Figure 2). Focal adhesion kinase (phospho-FAK Y397) was constitutively activated in all mesotheliomas. The NF2 was weakly expressed in most frozen tumours, in which the residual NF2 expression likely originated from nonneoplastic cells in the specimens, whereas expression was nearly undetectable in mesothelioma cell lines except for MESO257 (Figure 2).

We investigated the FAK–p53 interaction in mesothelioma cell lines by FAK and p53 immunoprecipitations, followed by FAK immunostaining (Figure 3). The p53 immunoprecipitations revealed a dominant FAK 130 kDa band in five mesothelioma cell lines, which was confirmed by FAK immunostaining in FAK immunoprecipitations (Figure 3).

FAK shRNA knockdown or kinase inhibition results in upregulation of p53. The *FAK shRNA*-mediated knockdown resulted in ~60–70% inhibition of FAK protein expression in MESO257 at 48 h and 96 h post infection (Figure 4A). Treatment with FAK inhibitor PF562271 decreased expression of phospho-FAK, phospho-MDM2, and MDM2 in MESO257 and MESO296 in a dose-dependent manner (Figure 4B and Supplementary Figure 1). Interestingly, *FAK shRNA* knockdown or activity inhibition induced two- to three-fold upregulation of phospho-p53 and p53, indicating that FAK regulates p53 (Figure 4). The p53 expression quantifications were normalised to control transfections using empty vector pLKO or DMSO.

Combination inhibition of the FAK–p53 and MDM2–p53 interactions suppressed cell viability in mesothelioma. Additive effects on p53 expression were obtained through coordinated dysregulation of p53, as demonstrated by immunoblots, after *FAK shRNA* knockdown and MDM2 inhibition. Inhibition of FAK–p53 and MDM2–p53 interactions were evaluated in five mesothelioma cell lines including MESO924, MESO257, MESO296, MESO428, and JMN1B, at 48 h after treatment with nutlin-3 and/or at 72 h post infection with *FAK shRNA* (Figure 5A). JMN1B is a control cell line, which has mutant/inactivated p53. The expression of MDM2, p53, and phospho-p53 increased in a dose-dependent manner after treatment with nutlin-3 in cells with wild type p53 (MESO924, MESO257, MESO296, and MESO428). Similarly, p53 expression and phosphorylation increased after *FAK shRNA* knockdown in these cells. Phospho-p53 and total p53 expression quantifications were normalised to DMSO-treated cells. Combination of FAK knockdown and MDM2–p53 inhibition by nutlin-3 induced greater p53, phospho-p53, and CDK inhibitor p21 expression, and inhibited proliferation marker cyclin A expression,

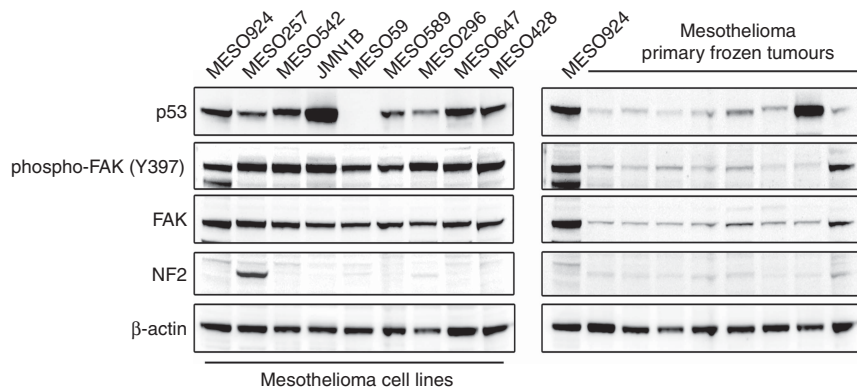


Figure 2. Immunoblotting evaluation of the phosphorylation and expression of FAK and p53 in mesothelioma total cell lysates. The left panel shows mesothelioma cell lines and the right panel shows primary frozen tumours. Both western blots include one epithelial-type mesothelioma (MESO924) for comparison. Actin staining is a loading control.

more effectively compared to either intervention alone (Figure 5A). By contrast, expression and phosphorylation of p53 did not increase in JMN1B after treatment with nutlin-3 and *FAK shRNA* either alone or in combination. However, *FAK shRNA* knockdown inhibited cyclin A proliferation marker expression in JMN1B cells (Figure 5A).

Additive effects on cell viability and cell cycle inhibition were obtained through coordinated dysregulation of p53 after FAK and MDM2 inhibition. *FAK* knockdown in wild-type p53 mesothelioma cell lines MESO924, MESO257, MESO296, and MESO428 resulted in ~15–35% inhibition of cell viability at 3 days after FAK silencing, compared with an empty vector control (Figure 5B). In p53 wild-type cells, the most striking reduction in cell viability

(20–50%) was seen after treatment with nutlin-3 (Figure 5B). However, viability was little affected in p53 mutant JMN1B cells after treatment with nutlin-3 (Figure 5B). To determine whether FAK kinase activity regulates mesothelioma viability, the FAK kinase was inactivated using a small molecule inhibitor, PF562271. Treatment with PF562271 showed profound anti-proliferative effects at day 6 in all the five mesothelioma cell lines (Figure 5C). Combination of *FAK shRNA* (day 3) or FAK inhibition (PF562271, day 6) and MDM2 inhibition resulted in 20–77% or 80–90% reduction in viability for these lines, respectively (Figure 5B and C). Interestingly, *FAK shRNA* knockdown or FAK kinase inhibition resulted in ~90% or 50% viability reduction in JMN1B cells, respectively (Figure 5B and C).

The FAK knockdown in all the five mesothelioma cell lines resulted in G1 arrest. The G1 peaks were 54% (MESO924), 52% (MESO257), 61% (MESO296), 48% (MESO428), and 36% (JMN1B) in the empty vector-treated cells compared with 64% (MESO924), 62% (MESO257), 70% (MESO296), 65% (MESO428), and 40% (JMN1B) in *FAK shRNA* knockdown cells (Figure 5D and Table 1). The cell cycle analyses also demonstrated a G1 block with a decrease in the S-phase population after MDM2 inhibition by nutlin-3 in wild-type p53 mesothelioma cell lines (Figure 5D and Table 1). The combination of *FAK shRNA* and MDM2 inhibition resulted in a G1/G2 block in cell cycle for these lines (Figure 5D and Table 1). The FAK knockdown also induced apoptosis in JMN1B: nuclear fragmentation was demonstrated in 4.6% cells treated with empty vector control, but in 13% cells treated with *FAK shRNA* (Figure 5D and Table 1).

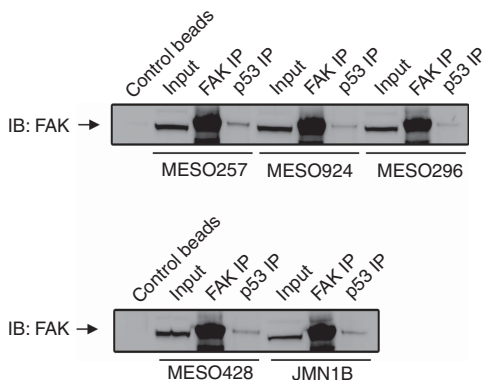


Figure 3. The FAK–p53 complex in mesothelioma cell lines. FAK–p53 interactions were evaluated by p53 immunoprecipitation followed by FAK immunoblotting.

NF2 regulates the FAK–p53 and MDM2–p53 interaction. The observations of mild upregulation of p53 by *FAK shRNA* knockdown in MESO257 (Figure 5A) with strong NF2 expression

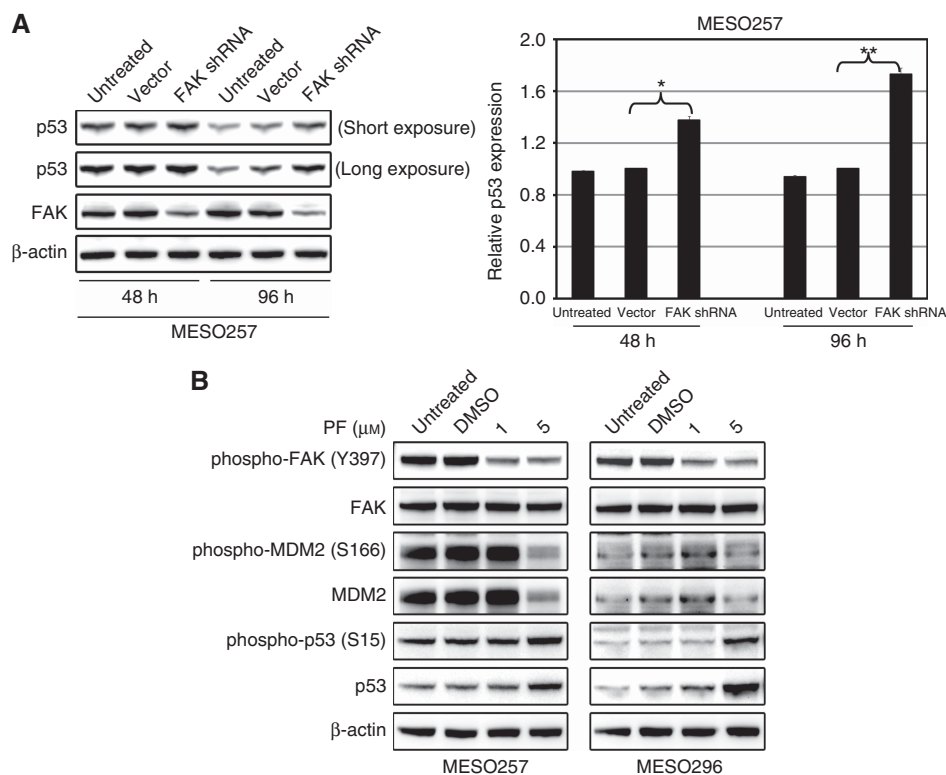


Figure 4. FAK silencing or inhibition induces p53 expression. (A) Left panel: Lentiviral *FAK shRNA* knockdown resulted in upregulation of p53 in MESO257 at 48 h and 96 h post infection. Right panel: quantification of p53 protein levels. The experiments were performed in triplicate, and statistically significant differences between vector control and *FAK shRNA* are defined as * $P < 0.05$, ** $P < 0.01$. (B) Expression of FAK, phospho-FAK, p53, phospho-p53, MDM2, and phospho-MDM2 was evaluated by immunoblotting in MESO257 and MESO296 after incubating cells for 6 h with FAK inhibitor PF562271 (1 and 5 μM) in serum-free medium. Actin staining is a loading control.

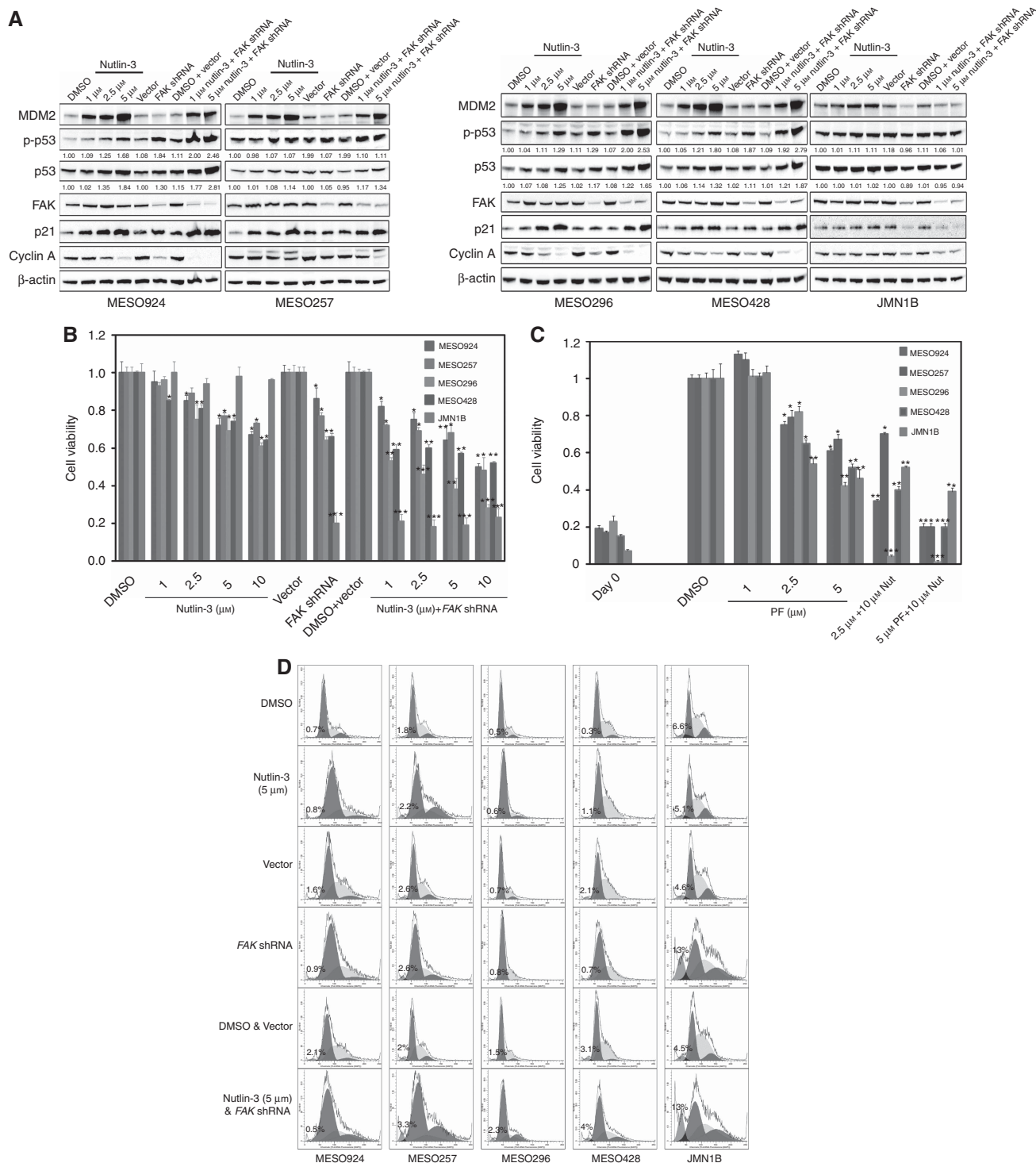


Figure 5. Additive effects of coordinated dysregulation of p53, as demonstrated by immunoblotting (**A**), cell viability (**B** and **C**) and cell cycle analyses (**D**), showing that FAK and MDM2 inhibition induced greater p53 expression, anti-proliferative effects, and cell cycle arrest, as compared to either intervention alone. (**A**) FAK, MDM2, phospho-p53, p53, p27, and cyclin A were evaluated by immunoblotting at 72 h post-infection with *FAK shRNA* and/or 48 h after treatment with nutlin-3. Actin staining is a loading control. Phospho-p53 and p53 expression quantitations are standardised to the DMSO or empty vector control. (**B** and **C**) Cell viability was evaluated by a Cell-titer Glo ATP-based luminescence assay in wild type p53 mesothelioma cell lines (MESO924, MESO257, MESO296, and MESO428), and in mutant p53 mesothelioma cell line (JMN1B), at 72 h post-infection with *FAK shRNA* and/or 48 h after treatment with nutlin-3 (**B**) or 6 days after treatment with nutlin-3 and PF562271 (**C**). Data were normalised to empty lentivirus infections or DMSO, and represent the mean values (\pm s.d.) from quadruplicate cultures. Statistically significant differences between untreated control and treatments or between empty vector control and *FAK shRNA* are presented as * $P < 0.05$, ** $P < 0.01$, *** $P < 0.001$. (**D**) Cell cycle analyses were performed 72 h after transduction with lentiviral *FAK shRNA* constructs and/or 48 h after treatment with nutlin-3. MESO924, MESO257, MESO296, MESO428, and JMN1B cells show substantial G1 and G2-block after *FAK* silencing and inhibition of the MDM2–p53 interaction, as compared with empty vector or DMSO control. JMN1B shows substantial nuclear fragmentation after *FAK* silencing.

Table 1. Cell cycle analysis after treatment with 5 μ M Nutlin-3, FAK shRNA, and combination in mesothelioma cell lines

	MESO924				MESO257				MESO296				MESO428				JMN1B			
	G _{1/0}	G ₂	S	A	G _{1/0}	G ₂	S	A	G _{1/0}	G ₂	S	A	G _{1/0}	G ₂	S	A	G _{1/0}	G ₂	S	A
DMSO	62	10	28	0.7	53	8	39	1.8	62	7	31	0.5	52	5	43	0.3	36	15	49	6.6
Nutlin-3	68	8	24	0.8	55	24	21	2.2	79	6	15	0.6	50	2	48	1.1	36	16	48	5.1
Vector	54	6	40	1.6	52	9	39	2.6	61	6	33	0.7	48	2	50	2.1	36	15	49	4.6
FAK shRNA	64	6	30	0.9	62	12	26	2.6	70	1	29	0.8	65	1	34	0.7	40	23	37	13
DMSO & Vector	54	6	40	2.1	51	9	40	2.0	63	5	32	1.5	52	3	45	3.1	37	10	53	4.5
Nutlin-3 & FAK shRNA	62	16	22	0.5	60	30	11	3.3	68	16	16	2.3	60	12	28	4.0	43	24	33	13

Abbreviations: DMSO = dimethyl sulphoxide; FAK = focal adhesion kinase; shRNA = short hairpin RNA. 'A': pre-G1. The data were obtained from Figure 5D and shown by percentage (%).

(Figure 2), as compared with strong induction of p53 expression after FAK knockdown in NF2-null mesothelioma cell lines (Figure 5A), suggests that the FAK–p53 interaction is regulated by NF2. The NF2 overexpression (wild-type and constitutive activated mutation *NF2 S518A*) inhibits FAK phosphorylation in NF2-null mesothelioma cell line (MESO924), but not loss-of-function mutant *NF2 S518D* (Supplementary Figure 2), which is in keeping with previous evidence for regulation of FAK activity by NF2 (Poulikakos *et al*, 2006). We therefore evaluated the interaction of NF2 with FAK in MESO257, which expresses NF2 strongly. The NF2–FAK interaction in MESO257 was evaluated by NF2 and FAK immunoprecipitations followed by NF2 and FAK immunoblotting (Figure 6A). The NF2 immunoprecipitations revealed a dominant FAK 130kDa band, and FAK IP revealed a weak NF2 band (Figure 6A). Co-localisation of NF2, FAK, p53, and MDM2 was evaluated by isolation of membrane, cytoplasm, and nucleus fractions in MESO257 (Figure 6B). The NF2, p53, and MDM2 are predominantly nuclear and partial FAK nuclear localisation was also confirmed by immunoblot (Figure 6B).

We next investigated whether NF2 and FAK silencing additively induces p53 expression in MESO257. The p53 expression quantifications were normalised to control infections using empty vector pLKO. The *NF2* and *FAK shRNA* knockdowns resulted in greater than 50% and 60% inhibition of expression of their targets. The *NF2 shRNA* knockdown induced p53, p21, and MDM2 expression, and FAK silencing resulted in upregulation of p53, p21, and p27. The combination of *FAK* and *NF2 shRNA* knockdowns increased p53, MDM2, p21, and p27 expression two- to three-fold, which was greater than the level after either intervention alone (Figure 6C). Furthermore, we investigated p53 and p21 expression in nuclear, cytoplasmic, and membrane fractions after NF2 knockdown (Figure 6D). The *NF2 shRNA* knockdown induced p53 in each of these subcellular fractions, at levels comparable to those in the total cell lysate. Similarly, p21 expression was induced in the nuclear and cytoplasmic fractions, at levels comparable to those in the total cell lysate (Figure 6D). In addition, NF2-positive MESO257 cells demonstrated increased sensitivity to FAK shRNA after NF2 knockdown (Figure 6E).

DISCUSSION

Mesothelioma is a fatal malignancy most often associated with asbestos exposure. Currently available therapies, which involve aggressive surgery, radiation, and chemotherapy, have done little to improve the prognosis of patients with this cancer. Incomplete understanding of mesothelioma biology has hindered the development of more effective therapeutics. Evidence indicates that activation of tyrosine kinases is essential in the progression from nonneoplastic mesothelial progenitor cells to mesothelioma. p53, a tumour suppressor, has a crucial role in the cellular responses to a variety of stresses, such as hypoxia or DNA damage, through its

accumulation in the nucleus (Levine, 1997; Oren, 1999). Inactivating *TP53* mutations are found in approximately 50% of human tumours (Hollstein *et al*, 1991). However, *TP53* mutations are seen less frequently in mesothelioma (Metcalf *et al*, 1992; Papp *et al*, 2001). Previous studies have suggested that p53 activity is potentially lost in mesothelioma because of p14ARF inactivation and the effects of the SV40 large T antigen (Testa and Giordano, 2001; Yang *et al*, 2001). However, the role of SV40 in mesothelioma carcinogenesis and the frequency of SV40 presence in mesothelioma have been questioned (Lopez-Rios *et al*, 2004; Whitson and Kratzke, 2006). Furthermore, recent studies indicate that p53 is functional in the absence of p14ARF and can induce apoptosis in mesothelioma (Hopkins-Donaldson *et al*, 2006). Thus, the identification of TK–p53 interactions and their functional evaluation in mesothelioma provides an opportunity to identify novel therapeutic strategies.

The interaction of tyrosine kinases and the p53 family was first reported by investigating the association of c-Abl and p73 α in apoptosis (Agami *et al*, 1999). In the present study, we identified a tyrosine kinase, FAK, that is highly expressed in mesothelioma, and investigated potential interactions of FAK with p53. Although interaction between FAK and p53 was shown previously by a biochemical approach (Golubovskaya *et al*, 2005), it is still unclear whether the FAK–p53 interaction may also have a crucial role in tumour biology. In previous studies, we developed and validated a functional proteomic approach including double phosphotyrosine and panRTK immuno-affinity purification, coupled to tandem mass spectrometry in various tumour tissues or cell lines (Ou *et al*, 2011). We therefore identified the interaction of FAK–p53 in the MESO257 cell line by the PY–p53 double purification and mass spectrometry approach (Figure 1), and validated this interaction in five mesothelioma cell lines by FAK and p53 immunoprecipitations (Figure 3). Immunoblotting evaluations of FAK and p53 expression and phosphorylation in mesothelioma cell lines and primary frozen tumours further demonstrated that FAK and p53 are ubiquitously expressed and constitutively activated in mesothelioma (Figure 2), indicating that FAK–p53 pathways have a role in mesothelioma growth. In addition, normal p53 expression in most mesothelioma samples confirmed that *TP53* mutations are infrequent in these cancers (Figure 2).

To evaluate whether FAK–p53 interaction has crucial functional roles in mesothelioma, FAK was silenced by lentiviral *FAK shRNA* in wild-type p53 mesothelioma cell lines (MESO924, MESO257, MESO296, and MESO428) and in the mutant p53 JMN1B line (Figures 4 and 5A). Interestingly, *FAK shRNA* knockdown induced one- to three-fold increases of p53 expression and phosphorylation in wild-type p53 mesothelioma cell lines, which is consistent with the level of p53 upregulation after *FAK shRNA* knockdown in human fibroblasts (Lim *et al*, 2008). The p53 expression did not increase after FAK inhibition at low concentrations of PF562271 (Supplementary Figure 1). Further studies showed that FAK inhibition at high concentration of PF562271 (5 μ M) induced p53

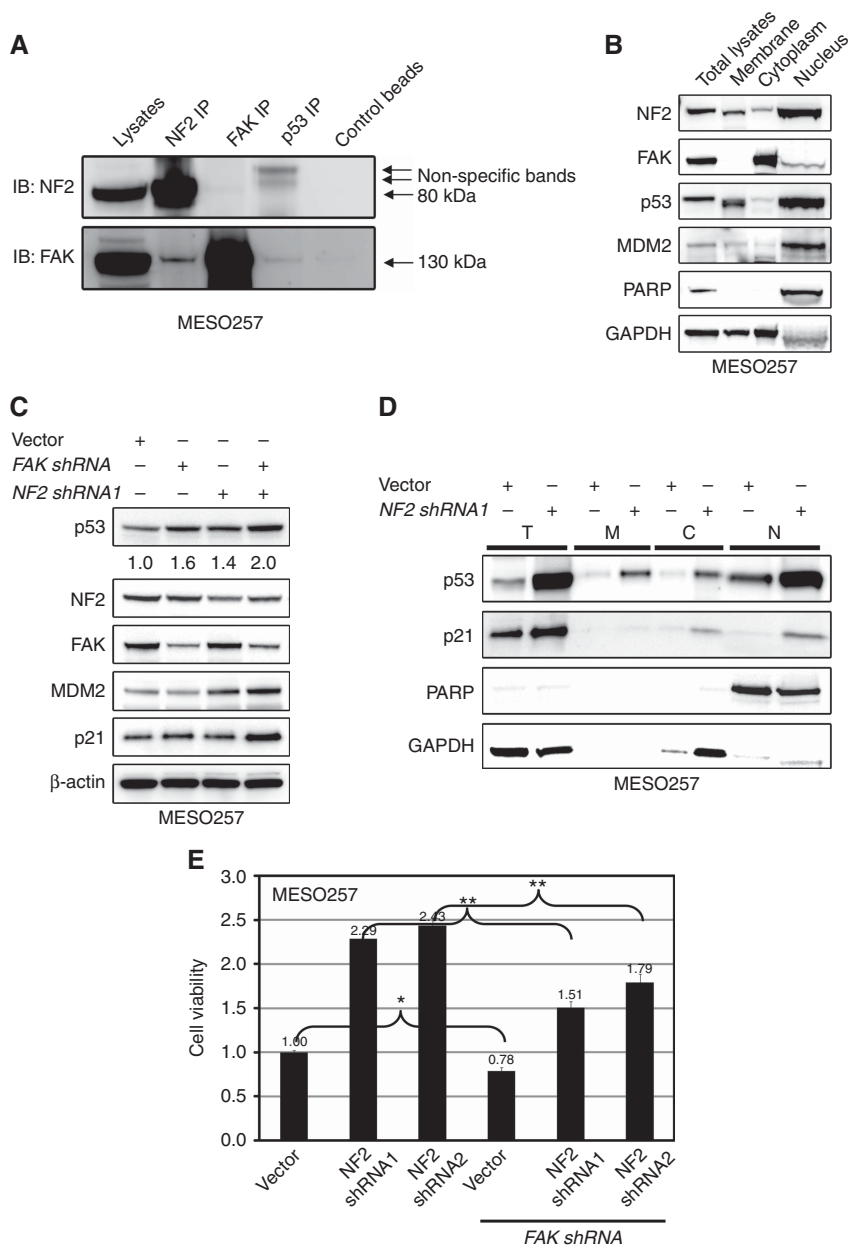


Figure 6. NF2 regulates the interaction of FAK–p53 and MDM2–p53. **(A)** The NF2–FAK complex was evaluated in MESO257 by NF2 and FAK immunoprecipitation followed by FAK and NF2 immunoblotting. **(B)** Nuclear localisation of NF2, FAK, p53, and MDM2 was evaluated in MESO257 by immunoprecipitation. Poly(ADP-ribose) polymerase (PARP) is a nuclear localisation control, and GAPDH is a cytoplasmic control. **(C)** In MESO257 with stable NF2 shRNA expression, p53, NF2, FAK, MDM2, and p21 expression were evaluated by immunoblotting after FAK shRNA knockdown for 72 h. beta-actin staining is a loading control. p53 expression quantifications are standardised to the empty vector control. **(D)** Expression of p53 and p21 was evaluated in MESO257 cell membrane, cytoplasm, and nucleus with stable NF2 shRNA expression by immunoblotting. **(E)** Cell viability was evaluated by a cell titre Glo ATP-based luminescence assay in MESO257 with stable expressed NF2 shRNA, at 72 h post-infection with FAK shRNA. Data were normalised to empty lentivirus infections, and represent the mean values (± s.d.) from quadruplicate cultures. Statistically significant differences between untreated control and treatments or between vector control and FAK shRNA or NF2 shRNA and NF2 + FAK shRNA are presented as **P*<0.05, ***P*<0.01.

expression because of inhibition of MDM2 and phospho-MDM2 expression (Figure 4B). These results are consistent with a FAK kinase-independent effect for p53 expression. However, FAK shRNA knockdown had little effect on p53 levels as compared with vector-treated cells in mutant p53 JMN1B cells (Figure 5A). These findings indicate that FAK negatively regulates wild-type p53 expression.

The structure and mechanisms of the MDM2–p53 interaction have been extensively studied (Kussie *et al*, 1996; Chene, 2003;

Brooks and Gu, 2006; White *et al*, 2006). MDM2 suppresses p53 activity by inducing nuclear export and degradation, and blocking its transcriptional activity (Chene, 2003). Therefore, inhibition of the wild-type p53–MDM2 interaction is an opportunity for cancer therapeutics (Kojima *et al*, 2006; Tovar *et al*, 2006; Van *et al*, 2009). In the current study, we show increased expression and phosphorylation of p53, and decreased viability in a dose-dependent manner after treatment with nutlin-3 in wild-type p53 cell lines (Figure 5A and B), indicating that inhibition of MDM2–p53

interaction has an important biological function in mesothelioma. It has been shown that FAK–p53 and MDM2–p53 form an autoregulatory feedback loop (Chene, 2003; Golubovskaya *et al*, 2005). The FAK shRNA knockdown induced expression of p53 and phospho-p53 (Figure 5A), which prevents association with MDM2 (Chene, 2003), but had little impact on MDM2 expression level (Figure 5A). By contrast, nutlin-3 treatment induced MDM2 and p53 expression, but had little effect on FAK expression in wild-type p53 mesothelioma cell lines. Nuclear FAK acts as a scaffold to stabilise the MDM2–p53 complex, leading to p53 polyubiquitination and subsequent p53 degradation by nuclear or cytoplasmic proteasomes (Lim *et al*, 2008). Those observations suggest that a feedback loop regulates FAK–p53–MDM2 activity. In the future, we will further study this signalling feedback loop in the tumour microenvironment.

The NF2 inactivation by genomic mechanisms occurs in more than 80% of mesothelioma, as a critical step in mesothelioma pathogenesis, and upregulates FAK activity (Bianchi *et al*, 1995; Poulidakos *et al*, 2006). A recent study showed that mesothelioma cells that are more sensitive to FAK inhibition lack NF2 expression (Shapiro *et al*, 2014). In the present study, in NF2-null MESO924, overexpression of mutant NF2 S518A, which mimics constitutively phosphorylated NF2 and functions equivalently to wild-type NF2, partially inhibited FAK activity, while overexpression of mutant, nonfunctional NF2 S518D, did not inhibit FAK activity (Supplementary Figure 2). The MESO257 cells showed strong NF2 expression, whereas NF2 expression was weak or nearly undetectable in the other mesothelioma cell lines and primary frozen tumours in this study (Figure 2), which is in keeping with previous evidence for NF2 inactivation by genomic mechanisms in mesothelioma (Metcalf *et al*, 1992; Papp *et al*, 2001). After treatment with nutlin-3, the FAK inhibitor PF562271, or FAK shRNA knockdown, upregulation of p53 and phospho-p53, and reduction of cell viability were least pronounced in NF2-positive MESO257 as compared with NF2-inactivated cell lines (Figure 5A–C), NF2 knockdown resulted in the accumulation of p53–p21 in nucleus and cytoplasm (Figure 6D), and NF2-positive MESO257 cells showed increased sensitivity to FAK shRNA after NF2 knockdown (Figure 6E), indicating that the presence of NF2 regulates MDM2–p53 and FAK–p53 interactions. This is in keeping with previous data demonstrating that NF2 neutralises the inhibitory effect of MDM2 on p53 (Kim *et al*, 2004), that NF2 negatively regulates FAK activity (Poulidakos *et al*, 2006), and that NF2 deficiency predicts increased sensitivity of mesothelioma cells to a FAK inhibitor, VS-4718 (Shapiro *et al*, 2014). NF2-null mesothelioma cells have been found to have weak cell–cell adhesions (Shapiro *et al*, 2014), which results in FAK leaving focal contact sites, increasing the cytoplasmic pool of FAK and enhancing FAK nuclear accumulation (Lim *et al*, 2008). Nuclear FAK acts as a scaffold to stabilise MDM2–p53 complexes, leading to p53 polyubiquitination and subsequent p53 degradation by nuclear or cytoplasmic proteasomes (Lim *et al*, 2008). These observations establish mechanisms by which FAK knockdown or FAK kinase activity inhibition suppress cell growth via minimising p53 degradation by MDM2 (Figure 4A and B, and Figure 5A), and have greater anti-proliferative effects in NF2-null mesothelioma cell lines (MESO296 and MESO428) than NF2-positive MESO257 cell lines (Figure 5B and C). Further, nuclear co-localisation of NF2, FAK, and p53 indicate that NF2 potentially regulates the interaction of FAK and p53 (Figure 6B). The NF2 shRNA knockdown resulted in the upregulation of p53 and MDM2 in MESO257 (Figure 6C), indicating that NF2 regulates the interaction of MDM2 and p53, and that upregulation of p53 expression by MDM2 inhibition (nutlin-3) is NF2-dependent. Focal adhesion kinase inhibits p53 through FAK nuclear translocation, binding to p53, and enhanced MDM2-dependent p53 ubiquitination and degradation (Lim *et al*, 2008). Thus, additive effects were obtained through coordinated reactivation of p53 by FAK knockdown, which attenuated MDM2-

dependent p53 degradation, and by NF2 knockdown, which attenuated the inhibitory effect of MDM2 on p53.

Our data indicate that FAK regulates cell survival via p53-dependent and -independent pathways, which was demonstrated by immunoblots after FAK knockdown in mutant p53 JMN1B cell line and in nonmutant p53 mesothelioma cell lines (MESO924, MESO257, MESO296, and MESO428; Figure 5). In addition, we found the dramatic anti-proliferative and apoptotic effects of FAK knockdown in mutant leiomyosarcoma cell lines (data not shown). The FAK (FAK shRNA or PF562271) and MDM2 (nutlin-3) inhibitors showed anti-proliferative effects in mesothelioma cell lines characterised by a decrease of cyclin A expression, CDK inhibitor p21 upregulation (Figure 5A), reduction of cellular viability (Figure 5B and C), and G1-phase arrest (Figure 5D). Interestingly, additive effects were obtained through a coordinated attack on p53, as demonstrated by immunoblots, cell viability, and cell cycle analyses, showing that FAK and MDM2 inhibition together induced greater p53 expression, cell apoptosis, anti-proliferative effects, and cell cycle arrest, as compared with either intervention alone. These findings highlight novel therapeutic opportunities in mesothelioma.

ACKNOWLEDGEMENTS

This study was supported by a grant from Zhejiang Provincial Top Key Discipline of Biology, the Major Science and Technology Special Project of Zhejiang Province (2012C03007-4, 2014C03004), the Natural Science Foundation of Zhejiang Province (LY13H160029), Science and Technology Bureau of Jiaying (2014AY21021), Science Foundation of Zhejiang Sci-Tech University (14042107-Y), China, and by the National Cancer Institute of the National Institutes of Health under Award Numbers 1P50CA127003 and 1P50CA168512.

CONFLICT OF INTEREST

The authors declare no conflict of interest.

AUTHOR CONTRIBUTIONS

W-BO and JAF designed the study. W-BO, ML, GE, JD, XM, YW, QH, QS, and H-MZ performed the experiments and acquired the data. W-BO, ML, GE, JD, XM, YW, QH, QS, H-MZ, and JAF analysed and interpreted the acquired data. W-BO, GE, and JAF participated in scientific discussion and drafting of the manuscript.

REFERENCES

- Agami R, Blandino G, Oren M, Shaul Y (1999) Interaction of c-Abl and p73alpha and their collaboration to induce apoptosis. *Nature* **399**(6738): 809–813.
- Bianchi AB, Mitsunaga SI, Cheng JQ, Klein WM, Jhanwar SC, Seizinger B, Kley N, Klein-Szanto AJ, Testa JR (1995) High frequency of inactivating mutations in the neurofibromatosis type 2 gene (NF2) in primary malignant mesotheliomas. *Proc Natl Acad Sci USA* **92**: 10854–10858.
- Bott M, Brevet M, Taylor BS, Shimizu S, Ito T, Wang L, Creaney J, Lake RA, Zakowski MF, Reva B, Sander C, Delsite R, Powell S, Zhou Q, Shen R, Olshen A, Rusch V, Ladanyi M (2011) The nuclear deubiquitinase BAP1 is commonly inactivated by somatic mutations and 3p21.1 losses in malignant pleural mesothelioma. *Nat Genet* **43**(7): 668–672.
- Brooks CL, Gu W (2006) p53 ubiquitination: Mdm2 and beyond. *Mol Cell* **21**(3): 307–315.

- Brummelkamp TR, Fabius AW, Mullenders J, Madiredjo M, Velds A, Kerkhoven RM, Bernards R, Beijersbergen RL (2006) An shRNA barcode screen provides insight into cancer cell vulnerability to MDM2 inhibitors. *Nat Chem Biol* 2(4): 202–206.
- Carbone M, Pass HI, Rizzo P, Marinetti M, Di Muzio M, Mew DJ, Levine AS, Procopio A (1994) Simian virus 40-like DNA sequences in human pleural mesothelioma. *Oncogene* 9: 1781–1790.
- Chene P (2003) Inhibiting the p53-MDM2 interaction: an important target for cancer therapy. *Nat Rev Cancer* 3(2): 102–109.
- Craighead JE, Mossman BT (1982) The pathogenesis of asbestos-associated diseases. *N Engl J Med* 306: 1446–1455.
- Demetri GD, Zenzie BW, Rheinwald JG, Griffin JD (1989) Expression of colony-stimulating factor genes by normal human mesothelial cells and human malignant mesothelioma cells lines *in vitro*. *Blood* 74: 940–946.
- Ding J, Huang S, Wu S, Zhao Y, Liang L, Yan M, Ge C, Yao J, Chen T, Wan D, Wang H, Gu J, Yao M, Li J, Tu H, He X (2010) Gain of miR-151 on chromosome 8q24.3 facilitates tumour cell migration and spreading through downregulating RhoGDI. *Nat Cell Biol* 12(4): 390–399.
- Ding Q, Grammer JR, Nelson MA, Guan JL, Stewart Jr JE, Gladson CL (2005) p27Kip1 and cyclin D1 are necessary for focal adhesion kinase regulation of cell cycle progression in glioblastoma cells propagated *in vitro* and *in vivo* in the scid mouse brain. *J Biol Chem* 280(8): 6802–6815.
- Gabarra-Niecko V, Schaller MD, Dunty JM (2003) FAK regulates biological processes important for the pathogenesis of cancer. *Cancer Metastasis Rev* 22(4): 359–374.
- Golubovskaya V, Kaur A, Cance W (2004) Cloning and characterization of the promoter region of human focal adhesion kinase gene: nuclear factor kappa B and p53 binding sites. *Biochim Biophys Acta* 1678(2–3): 111–125.
- Golubovskaya VM, Finch R, Cance WG (2005) Direct interaction of the N-terminal domain of focal adhesion kinase with the N-terminal transactivation domain of p53. *J Biol Chem* 280(26): 25008–25021.
- Golubovskaya VM, Finch R, Zheng M, Kurenova EV, Cance WG (2008) The 7-amino-acid site in the proline-rich region of the N-terminal domain of p53 is involved in the interaction with FAK and is critical for p53 functioning. *Biochem J* 411(1): 151–160.
- Hollstein M, Sidransky D, Vogelstein B, Harris CC (1991) p53 mutations in human cancers. *Science* 253: 49–53.
- Hopkins-Donaldson S, Belyanskaya LL, Simoes-Wust AP, Sigrist B, Kurtz S, Zangemeister-Wittke U, Stahel R (2006) p53-induced apoptosis occurs in the absence of p14(ARF) in malignant pleural mesothelioma. *Neoplasia* 8(7): 551–559.
- Huang J, Zheng DL, Qin FS, Cheng N, Chen H, Wan BB, Wang YP, Xiao HS, Han ZG (2010) Genetic and epigenetic silencing of SCARA5 may contribute to human hepatocellular carcinoma by activating FAK signaling. *J Clin Invest* 120(1): 223–241.
- Ilic D, Almeida EA, Schlaepfer DD, Dazin P, Aizawa S, Damsky CH (1998) Extracellular matrix survival signals transduced by focal adhesion kinase suppress p53-mediated apoptosis. *J Cell Biol* 143(2): 547–560.
- Iwahori K, Serada S, Fujimoto M, Nomura S, Osaki T, Lee CM, Mizuguchi H, Takahashi T, Ripley B, Okumura M, Kawase I, Kishimoto T, Naka T (2011) Overexpression of SOCS3 exhibits preclinical antitumor activity against malignant pleural mesothelioma. *Int J Cancer* 129(4): 1005–1017.
- Janne PA, Taffaro ML, Salgia R, Johnson BE (2002) Inhibition of epidermal growth factor receptor signaling in malignant pleural mesothelioma. *Cancer Res* 62(18): 5242–5247.
- Jongsma J, van Montfort E, Vooijs M, Zevenhoven J, Krimpenfort P, van der Valk M, van de Vijver M, Berns A (2008) A conditional mouse model for malignant mesothelioma. *Cancer Cell* 13(3): 261–271.
- Kim H, Kwak NJ, Lee JY, Choi BH, Lim Y, Ko YJ, Kim YH, Huh PW, Lee KH, Rha HK, Wang YP (2004) Merlin neutralizes the inhibitory effect of Mdm2 on p53. *J Biol Chem* 279(9): 7812–7818.
- Kojima K, Konopleva M, McQueen T, O'Brien S, Plunkett W, Andreeff M (2006) Mdm2 inhibitor Nutlin-3a induces p53-mediated apoptosis by transcription-dependent and transcription-independent mechanisms and may overcome Atm-mediated resistance to fludarabine in chronic lymphocytic leukemia. *Blood* 108(3): 993–1000.
- Kussie PH, Gorina S, Marechal V, Elenbaas B, Moreau J, Levine AJ, Pavletich NP (1996) Structure of the MDM2 oncoprotein bound to the p53 tumor suppressor transactivation domain. *Science* 274(5289): 948–953.
- Levine AJ (1997) p53, the cellular gatekeeper for growth and division. *Cell* 88(3): 323–331.
- Li Q, Kawamura K, Yamanaka M, Okamoto S, Yang S, Yamauchi S, Fukamachi T, Kobayashi H, Tada Y, Takiguchi Y, Tatsumi K, Shimada H, Hiroshima K, Tagawa M (2012) Upregulated p53 expression activates apoptotic pathways in wild-type p53-bearing mesothelioma and enhances cytotoxicity of cisplatin and pemetrexed. *Cancer Gene Ther* 19(3): 218–228.
- Lim ST, Chen XL, Lim Y, Hanson DA, Vo TT, Howerton K, Larocque N, Fisher SJ, Schlaepfer DD, Ilic D (2008) Nuclear FAK promotes cell proliferation and survival through FERM-enhanced p53 degradation. *Mol Cell* 29(1): 9–22.
- Long W, Yi P, Amazit L, LaMarca HL, Ashcroft F, Kumar R, Mancini MA, Tsai SY, Tsai MJ, O'Malley BW (2010) SRC-3Delta4 mediates the interaction of EGFR with FAK to promote cell migration. *Mol Cell* 37(3): 321–332.
- Lopez-Rios F, Illei PB, Rusch V, Ladanyi M (2004) Evidence against a role for SV40 infection in human mesotheliomas and high risk of false-positive PCR results owing to presence of SV40 sequences in common laboratory plasmids. *Lancet* 364(9440): 1157–1166.
- Melkounian ZK, Peng X, Gan B, Wu X, Guan JL (2005) Mechanism of cell cycle regulation by FIP200 in human breast cancer cells. *Cancer Res* 65(15): 6676–6684.
- Metcalfe RA, Welsh JA, Bennett WP, Seddon MB, Lehman TA, Pelin K, Linnainmaa K, Tammilehto L, Mattson K, Gerwin BI. (1992) p53 and Kirsten-ras mutations in human mesothelioma cell lines. *Cancer Res* 52(9): 2610–2615.
- Moran DM, Maki CG (2010) Nutlin-3a induces cytoskeletal rearrangement and inhibits the migration and invasion capacity of p53 wild-type cancer cells. *Mol Cancer Ther* 9(4): 895–905.
- Oren M (1999) Regulation of the p53 tumor suppressor protein. *J Biol Chem* 274(51): 36031–36034.
- Ou WB, Corson JM, Flynn DL, Lu WP, Wise SC, Bueno R, Sugarbaker DJ, Fletcher JA (2011) AXL regulates mesothelioma proliferation and invasiveness. *Oncogene* 30(14): 1643–1652.
- Ou WB, Zhu J, Eilers G, Li X, Kuang Y, Liu L, Marino-Enriquez A, Yan Z, Li H, Meng F, Zhou H, Sheng Q, Fletcher JA (2015) HDACi inhibits liposarcoma via targeting of the MDM2-p53 signaling axis and PTEN, irrespective of p53 mutational status. *Oncotarget* 6(12): 10510–10520.
- Papp T, Schipper H, Pemsel H, Bastrop R, Muller KM, Wiethege T, Weiss DG, Dopp E, Schiffmann D, Rahman Q (2001) Mutational analysis of N-ras, p53, p16INK4a, p14ARF and CDK4 genes in primary human malignant mesotheliomas. *Int J Oncol* 18(2): 425–433.
- Parsons JT (2003) Focal adhesion kinase: the first ten years. *J Cell Sci* 116 (Pt 8): 1409–1416.
- Poulikakos PI, Xiao GH, Gallagher R, Jablonski S, Jhanwar SC, Testa JR (2006) Re-expression of the tumor suppressor NF2/merlin inhibits invasiveness in mesothelioma cells and negatively regulates FAK. *Oncogene* 25(44): 5960–5968.
- Rubin BP, Singer S, Tsao C, Duensing A, Lux ML, Ruiz R, Hibbard MK, Chen CJ, Xiao S, Tuveson DA, Demetri GD, Fletcher CD, Fletcher JA (2001) KIT activation is a ubiquitous feature of gastrointestinal stromal tumors. *Cancer Res* 61(22): 8118–8121.
- Schon O, Friedler A, Bycroft M, Freund SM, Fersht AR (2002) Molecular mechanism of the interaction between MDM2 and p53. *J Mol Biol* 323(3): 491–501.
- Shapiro IM, Kolev VN, Vidal CM, Kadariya Y, Ring JE, Wright Q, Weaver DT, Menges C, Padval M, McClatchey AI, Xu Q, Testa JR, Pachter JA (2014) Merlin deficiency predicts FAK inhibitor sensitivity: a synthetic lethal relationship. *Sci Transl Med* 6(237): 237ra68.
- Slack-Davis JK, Hershey ED, Theodorescu D, Frierson HF, Parsons JT (2009) Differential requirement for focal adhesion kinase signaling in cancer progression in the transgenic adenocarcinoma of mouse prostate model. *Mol Cancer Ther* 8(8): 2470–2477.
- Testa JR, Cheung M, Pei J, Below JE, Tan Y, Sementino E, Cox NJ, Dogan AU, Pass HI, Trusa S, Hesdorffer M, Nasu M, Powers A, Rivera Z, Comertpay S, Tanji M, Gaudino G, Yang H, Carbone M (2011) Germline BAP1 mutations predispose to malignant mesothelioma. *Nat Genet* 43(10): 1022–1025.
- Testa JR, Giordano A (2001) SV40 and cell cycle perturbations in malignant mesothelioma. *Semin Cancer Biol* 11(1): 31–38.
- Tovar C, Rosinski J, Filipovic Z, Higgins B, Kolinsky K, Hilton H, Zhao X, Vu BT, Qing W, Packman K, Myklebost O, Heimbrook DC, Vassilev LT (2006) Small-molecule MDM2 antagonists reveal aberrant p53 signaling in cancer: implications for therapy. *Proc Natl Acad Sci USA* 103(6): 1888–1893.

- Van MT, Ferdinande L, Taideman J, Lambertz I, Yigit N, Vercruyse L, Rihani A, Michaelis M, Cinatl Jr J, Cuvelier CA, Marine JC, De PA, Bracke M, Speleman F, Vandesompele J (2009) Antitumor activity of the selective MDM2 antagonist nutlin-3 against chemoresistant neuroblastoma with wild-type p53. *J Natl Cancer Inst* **101**(22): 1562–1574.
- White DE, Talbott KE, Arva NC, Bargonetti J (2006) Mouse double minute 2 associates with chromatin in the presence of p53 and is released to facilitate activation of transcription. *Cancer Res* **66**(7): 3463–3470.
- Whitson BA, Kratzke RA (2006) Molecular pathways in malignant pleural mesothelioma. *Cancer Lett* **239**(2): 183–189.
- Yang CT, You L, Uematsu K, Yeh CC, McCormick F, Jablons DM (2001) p14(ARF) modulates the cytolytic effect of ONYX-015 in mesothelioma cells with wild-type p53. *Cancer Res* **61**(16): 5959–5963.
- Zhao J, Pestell R, Guan JL (2001) Transcriptional activation of cyclin D1 promoter by FAK contributes to cell cycle progression. *Mol Biol Cell* **12**(12): 4066–4077.
- Zhou S, Liu L, Li H, Eilers G, Kuang Y, Shi S, Yan Z, Li X, Corson JM, Meng F, Zhou H, Sheng Q, Fletcher JA, Ou WB (2014) Multipoint targeting of the PI3K/mTOR pathway in mesothelioma. *Br J Cancer* **110**(10): 2479–2488.

This work is published under the standard license to publish agreement. After 12 months the work will become freely available and the license terms will switch to a Creative Commons Attribution-NonCommercial-Share Alike 4.0 Unported License.

Supplementary Information accompanies this paper on British Journal of Cancer website (<http://www.nature.com/bjc>)